Class: Four
Subject: Mechanics of Artificial Organs 2
Lecturer: Dr. Ameen M. Al-Juboori
E-mail: AmeenAL-Juboori@mustaqbal-college.edu.iq

Lecture # 4

Design of the Total Artificial Heart

1. Pump selection

1.1 Pulsatile Flow Pumps (Reciprocating Pumps and Rotary Displacement Pumps)

A pulsatile flow pump keeps a flow rate of a patient by driving a certain amount of blood, such as 70 mL, with a stroke. A sack type squeezes and expands a polymer sack pneumatically, namely by compressed/depressed air, or hydraulically, namely by silicone oil. A pusher plate type squeezes and expands a polymer sack with hard plates driven by an electromagnet or a motor/ball screw mechanism.

Since rotary displacement pumps, such as a roller pump or a tube pump, generate pulsatile flow, they are often classified as pulsatile flow pumps. In this type of pump, several rollers squeeze a tube and propel the blood forward. They have been used often in open heart surgery since only a tube is necessary for a patient.

1.2 Continuous Flow Pumps (Rotary Pumps or Turbo Pumps)

A “centrifugal pump” utilizes the outer pressure rise of a swirl (Figure 1). As long as the rotational speed of swirl is maintained, it generates a certain pressure without regard to flow rate.

On the other hand, an “axial flow pump” changes the flow orientation by airfoils and obtains a pressure as a reaction force, which subsequently forms a swirl (Figure 1). Since at a high flow rate the relative inflow angle becomes small, like a windmill, and a pressure becomes low and a higher rotational speed becomes necessary for high flow rates.

As long as the rotational speed of a rotary pump is maintained, a certain pressure rise is maintained even the external resistance, such as the aortic

valve resistance, is changed. It results in the pulsatility of blood flow as shown in Figure 2.

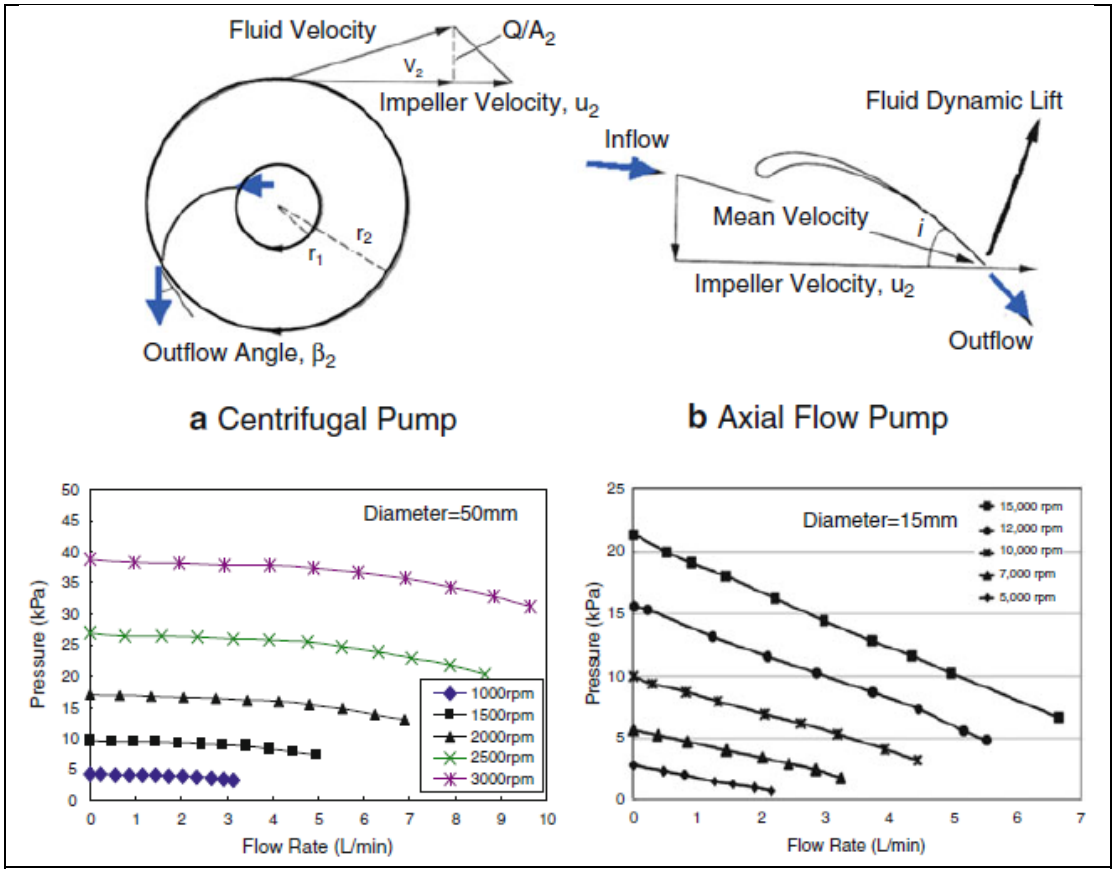

Figure 1: Centrifugal pump and axial flow pump

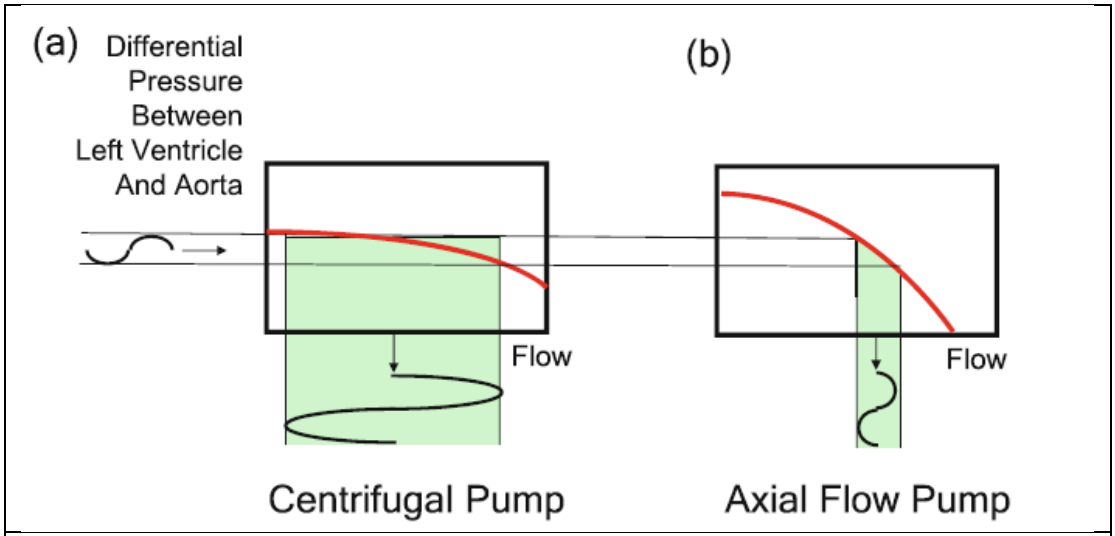

Figure 2: Pulsatility of rotary pumps

Though both types generate a pressure by making a swirl, there is a design continuity. The intermediate pump configuration between a centrifugal pump and an axial-flow pump is called “a mixed flow pump”. In the industrial pump designs, a parameter named “specific speed” is often referred (Figure 3). Specific speed is defined by

$$n_S \equiv \omega Q^{1/2} H^{-3/4}$$

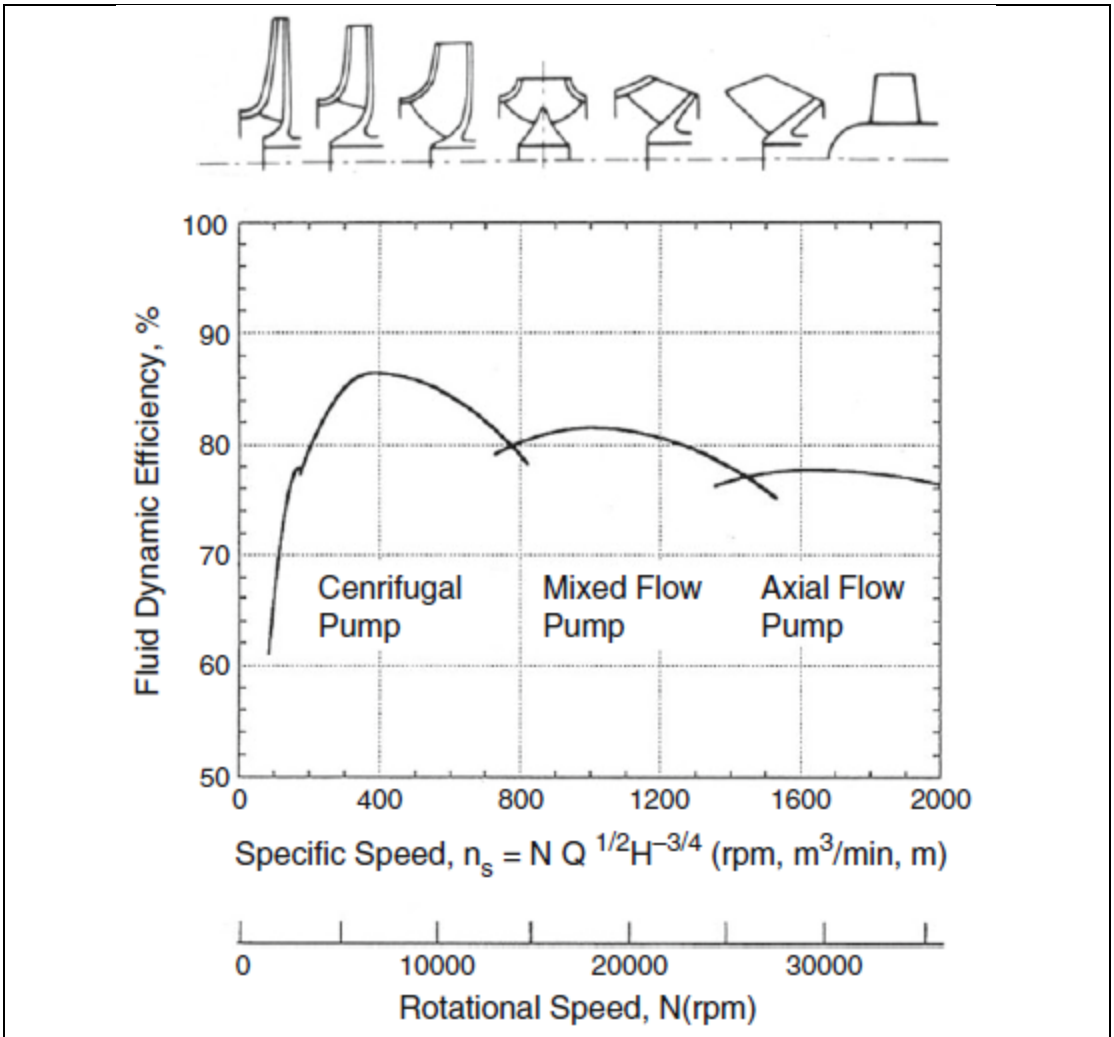

Figure 3: Selection of pump types

Where ω denotes angular velocity, Q flow rate, and H pressure head, respectively. When

$$gH = p/\rho = \eta(\omega R)^2$$

Is inserted from pump theory using efficiency, η, and gravity, g,

$$n_S{}^2 = (g/\eta)^{3/2}\left(Q/R^2\right)/(\omega R)$$

Since g/η is constant, it can be seen that the square of specific speed represents a ratio of [radial or axial velocity/tangential velocity].

The required performances to VAD pumps are as follows

1. Mean pressure rise of 100 mmHg (80–120 mmHg) for left ventricular assist.
2. Mean pressure rise of 20 mmHg (15–25 mmHg) for right ventricular assist.
3. Mean blood flow rate of 5 L/min (2–10 L/min) for full support for an adult at a rest.

2. Selection of Bearing Types

2.1 Pivot Bearing

The second generation implantable VADs are mostly axial flow pumps whose impellers are supported with mechanical bearings, especially with pivot bearings (Figure 4). The typical VADs are the JarvikHeart 'Jarvik-2000', the Thoratec 'HeartMate-II', and the ReliantHeart 'HeartAssist 5'. In the field of extracorporeal centrifugal pumps, such as Maquet 'Rotaflow' or Senko Medical 'MERA centrifugal pump, their impellers are supported with a single pivot, which is a so-called monopivot bearing.

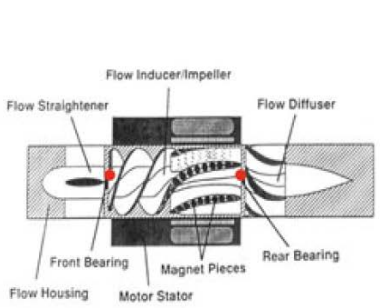

Axial flow pump with pivot bearings (as Thoratec HeartMate II; ReliantHeart HeartAssist 5; JarvikHeart Jarvik 2000)

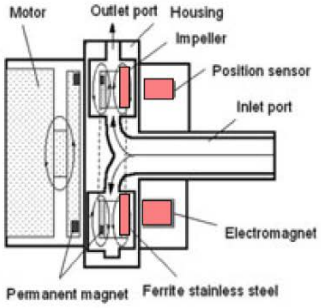

Axial magnetic bearing with 3 position sensors (as Terumo DuraHeart)

Centrifugal pump with hydrodymanic bearing (as HeartWare HVAD)

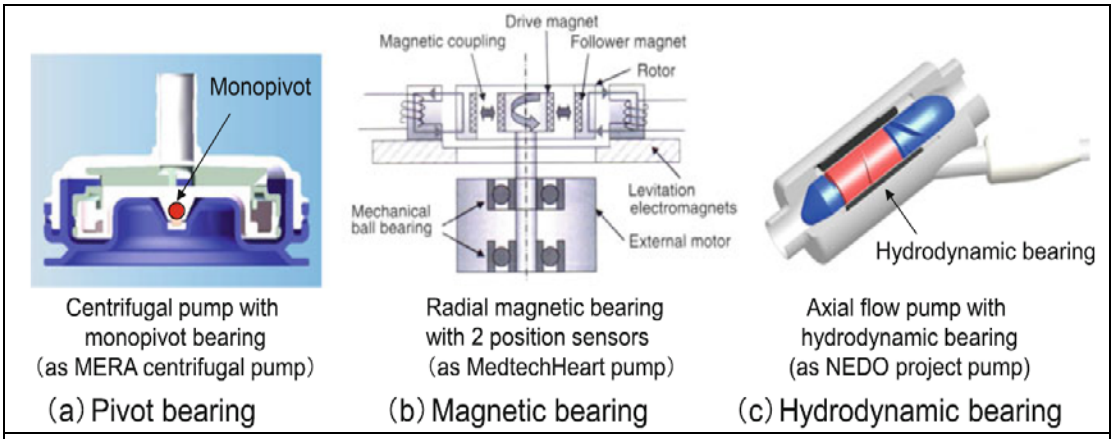

Figure 4: Classification of bearing types

For a pivot bearing, the wear, hemolysis, and thrombus formation at the pivot should be avoided. In a case of axial magnetic flux coupling, Dr. O. Maruyama showed experimentally the hemolysis depends on the contact areas using a monopivot centrifugal pump (Figure 5). In a case of radial magnetic flux coupling, we recently found the hemolysis was not so dependent to contact areas using a centrifugal pump without vanes or an outlet (Figure 6). The hemolysis index, NIH, is roughly a time gradient of plasma free hemoglobin, whose detail will be discussed later. Though these results showed a contrast, we should consider simultaneously the effect of magnetic forces.

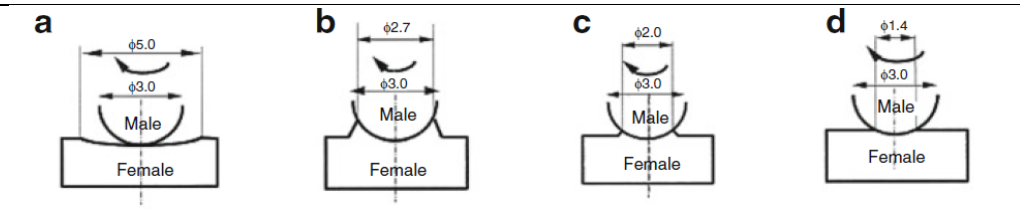

Hemolysis index, NIH, of centrifugal pumps (g/100L)

Pivot Shape	NIH of each test pump	NIH of a commercial centrifugal pump	Relative index
a	0.001	0.003	0.3
b	0.010	0.003	3.3
c	0.012	0.004	3.0
d	0.002	0.002	1.0

Figure 5: Effect of contact area of pivot bearings on hemolysis for a centrifugal pump with an axial flux coupling

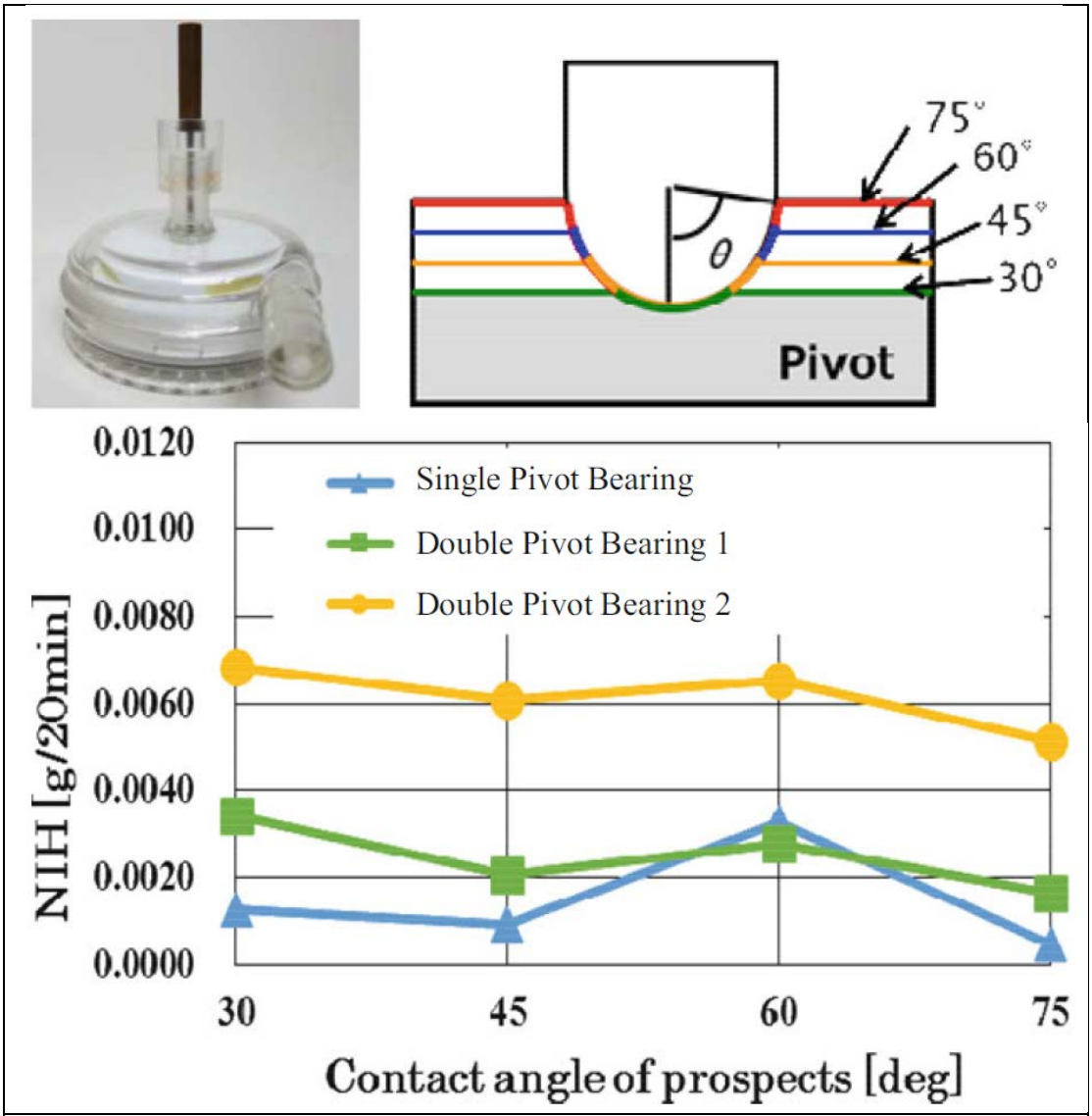

Figure 6: Effect of contact area of pivot bearings on hemolysis for a centrifugal pump with a radial flux coupling

2.2 Magnetic Bearing and Hydrodynamic Bearing

The third generation implantable VADs are mostly centrifugal pumps with non-contact bearings. There are two types for non-contact bearings: one is a magnetic bearing and the other is a hydrodynamic bearing (Figure 1).

The magnetic bearing is composed of stator coils and position sensors to maintain the rotor at a position. If the position sensor is axial, three sensors are necessary to maintain a rotating plane. If the position sensor is radial and the axial position is maintained by magnets, only two sensors are

necessary to maintain the rotor at the center, as shown in Figure 1-b. The motor mechanism is generally implemented separately.

The hydrodynamic bearing utilizes locally high pressures generated by fluid squeezed into a wedge-shaped channel or a step channel composed of relatively moving surfaces. An example of hydrodynamic bearing design is shown in Figure 7. As mentioned, the third generation devices consist of implantable rotary VADs with non-contact bearings. The Terumo 'DuraHeart' utilizes a magnetic bearing on the front side and a motor on the rear side. The SunMedical 'EVAHEART' utilizes a mechanical seal, separating blood and water with a submicron water film, and also a hydrodynamic bearing for motor axis. The HeartWare 'HVAD' utilizes hydrodynamic bearings and with magnetic suspension.

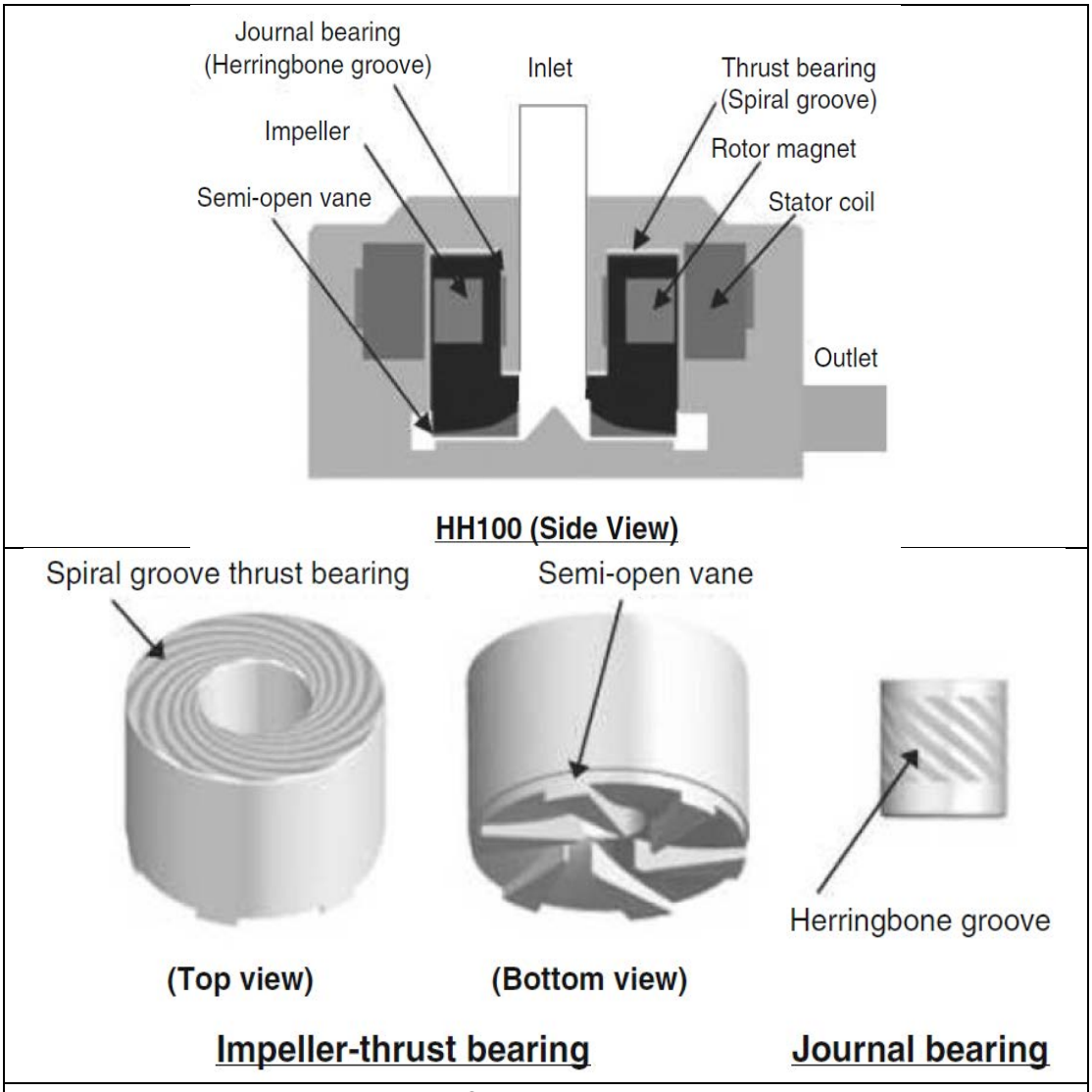

Figure 7: A design example of a hydrodynamic bearing pump.

As bridge-to-decision devices, high-performance rotary pumps have also emerged. Among them is a magnetic-bearing centrifugal pump, the Thoratec 'CentriMag', which can be used over several months.

3. Motor, Battery, and Magnetic Suspension

3.1 Motor Mechanism

A driving motor is also an important component. Brushless DC motors are most frequently applied to VADs. In the brushless DC motor, the stator is composed of coils rotating a magnetic field and the rotor is composed of permanent magnets. The way of switching current to form a rotating pair of poles is shown in Figure 8. It can be recognized that only a pair of coils is activated simultaneously. To prevent cogging, namely fluctuation of rotational speed, the numbers of rotor/stator poles are selected to be different such as 6-poles for a stator and 8-poles for a rotor.

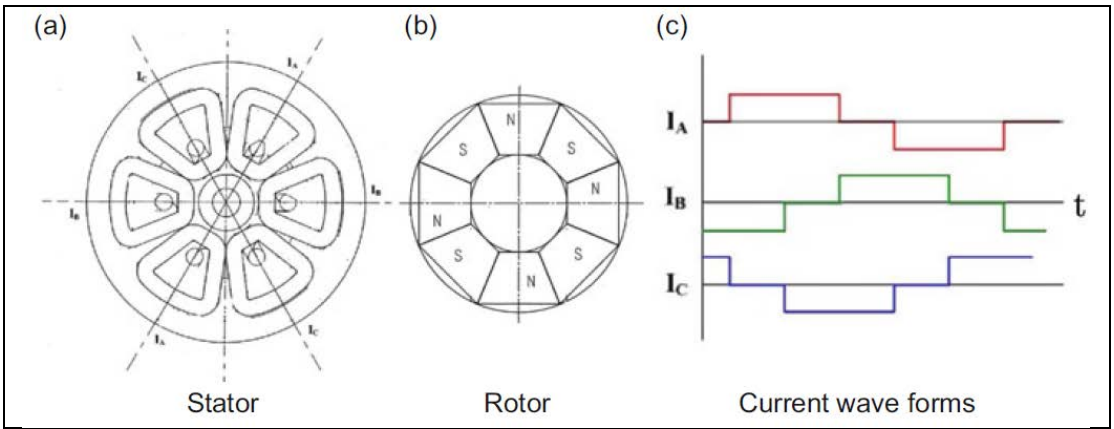

Figure 8: Mechanism of a brushless DC motor

3.2 Battery and Cable

Most of VADs have a power source composed of lithium-ion or nickel-cadmium battery. A patient often carries two batteries when he/she goes out and simultaneously two batteries are being charged at home.

Cables are designed as soft as possible to be easily bent but as strong as possible not to be broken by fatigue. Since cable infection is a severe clinical problem, the cable should not have gaps between skins at the penetration port.

Therefore a wireless transcutaneous energy transmission system, TETS, is requested from clinical side. However, it is not so easy to keep sufficient reliability and anatomical fit compared with a wired system. Sooner or later VADs with TETS would be provided by some manufacturers.

3.3 Magnetic Suspension

When we use permanent magnet for magnetic coupling or for magnetic suspension, we should understand an important theorem. Anything cannot be supported only by permanent magnets freely in a three-dimensional space without any stabilization control or without super conductivity. This is called as Earnshaw's theorem in magnetic fields. When we use rare-earth permanent magnets such as Nd-Fe-B, Sm-Co, we should be careful to their strong magnetic force. We should understand not only the radial repulsive force but also special axial force behavior such as shown in Figure 9.

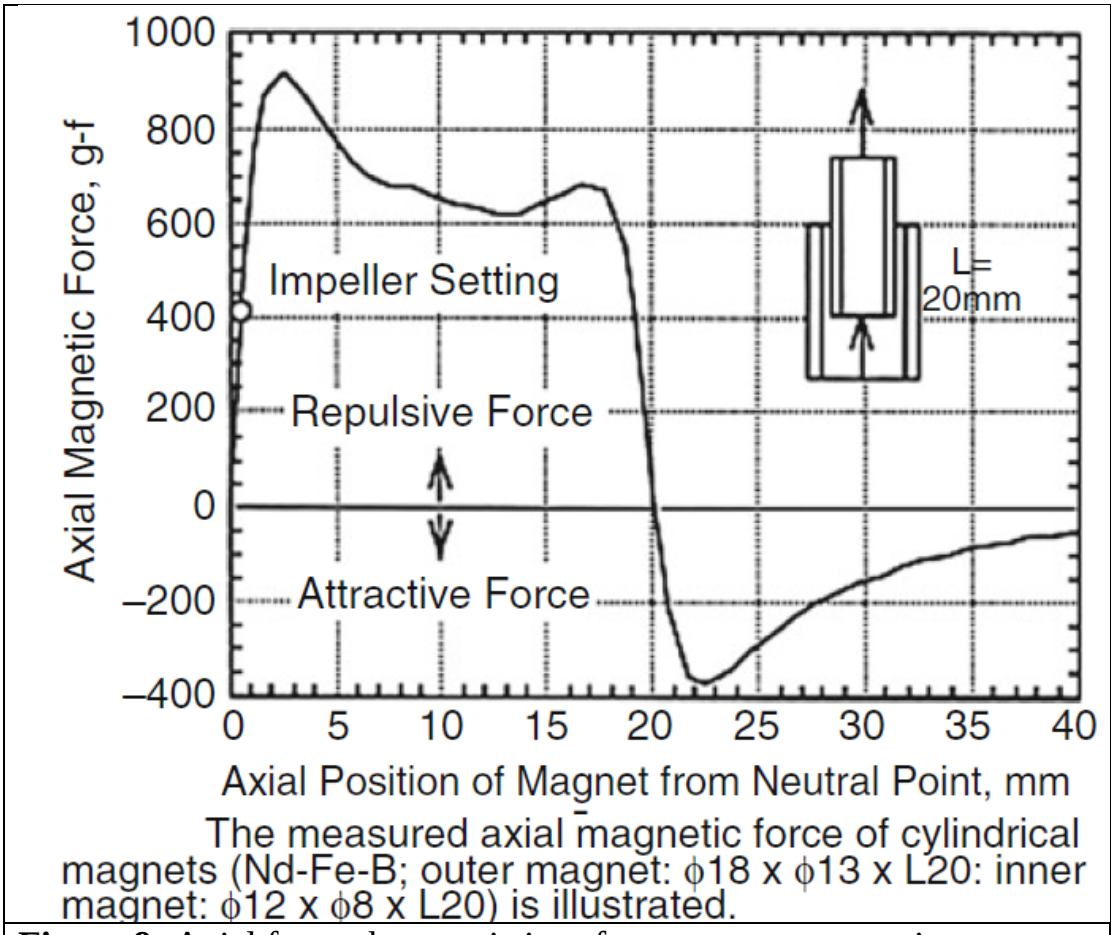

Figure 9: Axial force characteristics of permanent magnet rings

4. Flow Visualization and Computational Fluid Dynamic Analysis

4.1 Particle Image Velocimetry (PIV)

Flow visualization reveals the environments where blood is exposed. Though the tracer particles do not indicate the behavior of blood cells, they show flow velocity correctly when the size is as small as to trace the streamlines.

Apparatus (Figure 10): The pump model is filled with 64 % NaI water solution with a matched refractive index to acrylic resin (being 1.49). The images of SiO2 beads (0.15-mm sphere), having the same density as the liquid (1.9×10^3 kg/m^3), are suspended in the circuit. One of the imaging methods is to use double-pulse YAG laser with a short interval such as 1 μs interval and to transfer the two images to continuous two frames of regular video camera (with 1/30 s frame interval).

Another imaging method, for a particle tracking method, is to use a high-speed video camera (e.g., a frame rate of 4500 frame/s), and the particles are illuminated by a continuous laser light sheet

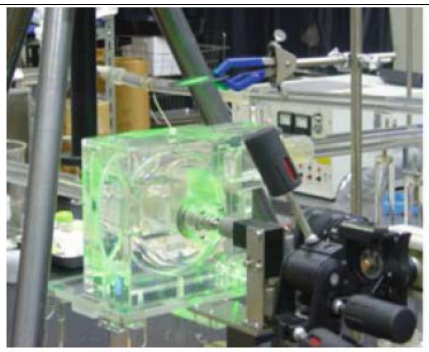

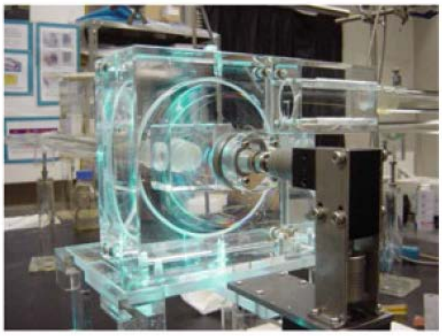

Apparatus	Acrylic 2.5x model
	Video camera (30frame/s)
	Double pulse YAG laser sheet (500μs)
Fluid	64wt%NaI aq (refluctive index: 1.49, specific gravity: 1.9)
Tracer	Silver coated glass beads (ϕ10 μm)
Analysis	Cross-correlation method

Apparatus	Acrylic 2.5x model
	High-speed Video camera (4500f/s, ring)
	Ar-ion laser light sheet (3-4W)
Fluid	64wt%NaI aq (refluctive index: 1.49, specific gravity: 1.9)
Tracer	SiO_2 beads (ϕ150 μm)
Analysis	4-frame particle tracking method

Figure 10: Experimental apparatus for flow visualization, (a) with a double-pulse laser (b) with a continuous laser

4.2 Visualization of a Centrifugal Blood Pump

Similarity law: A 300% scale-up visualization model is made with acrylic resin and is based on Reynolds similarity law, especially regarding the blood contacting geometry. The surface of the model is polished to the roughness of Ra<0.2 μm. The experimental conditions should be set based on the strict Reynolds similarity law, namely a 1/15 rotational speed and a 1.8× flow rate.

Particle image analysis (Figure 11): A method of analysis is a particle tracking velocimetry (PTV). (a) The four-frame tracking method can be used for in-plane motion to eliminate inaccurate particle images that cannot be traced for continuous four frames. A PTV has a fine spatial resolution even near the surface wall. (b) The three-frame tracking method or the spring-model tracking method can be used to evaluate the secondary flow of out-of-plane motion since particle images are captured only for two or three frames during penetration of the laser light sheet, whose thickness is 1.6 mm.

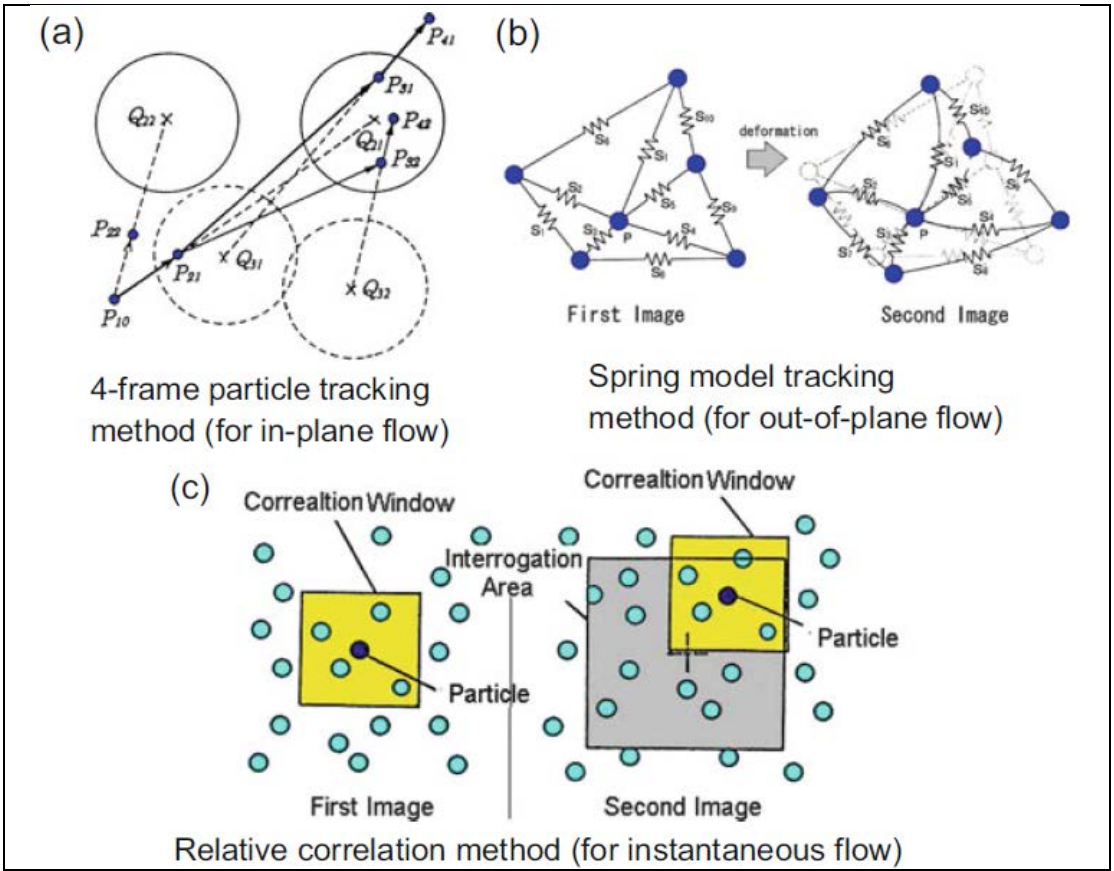

Figure 11: Analyses for particle image velocimetry (PIV)

(c) The other is a particle image correlation velocimetry (called PICV here), which finds the highest correlation points for several particles and derives a vector averaging several particles. Regarding the necessary resolution, the resolution was tuned up to obtain the sufficient contours of shear rate as shown in Results.

Sample results are shown here for a centrifugal pump. In the planar view from the tip of vanes to a volute, a flow from a vane is visualized to land smoothly on the surface of a casing or a volute (Figure 12). In the vertical view from the tip of vanes to a volute, a formation of a jet from a vane is well visualized.

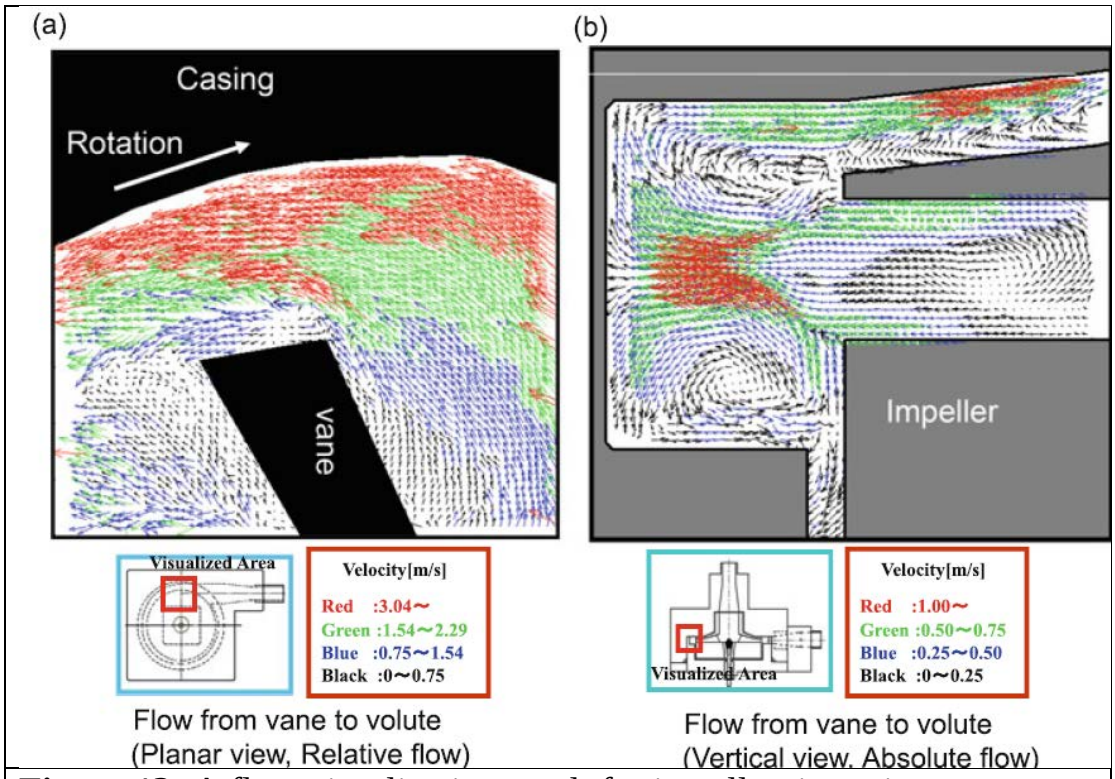

Figure 12: A flow visualization result for impeller tip region.

At the bifurcation point to the outlet, so-called a tongue, flow separation should be avoided. In a case of a separation, standing vortex is observed at the tongue region in flow visualization, shown in left part of Figure 13; correspondingly a thrombus is formed along volute surface from the tongue in an animal test. It can be removed by a design of round tongue, as shown in right part of Figure 13, then thrombus formation was avoided in an animal test. It indicates that flow visualization can estimate thrombus formation point but cannot estimate thrombus growth.

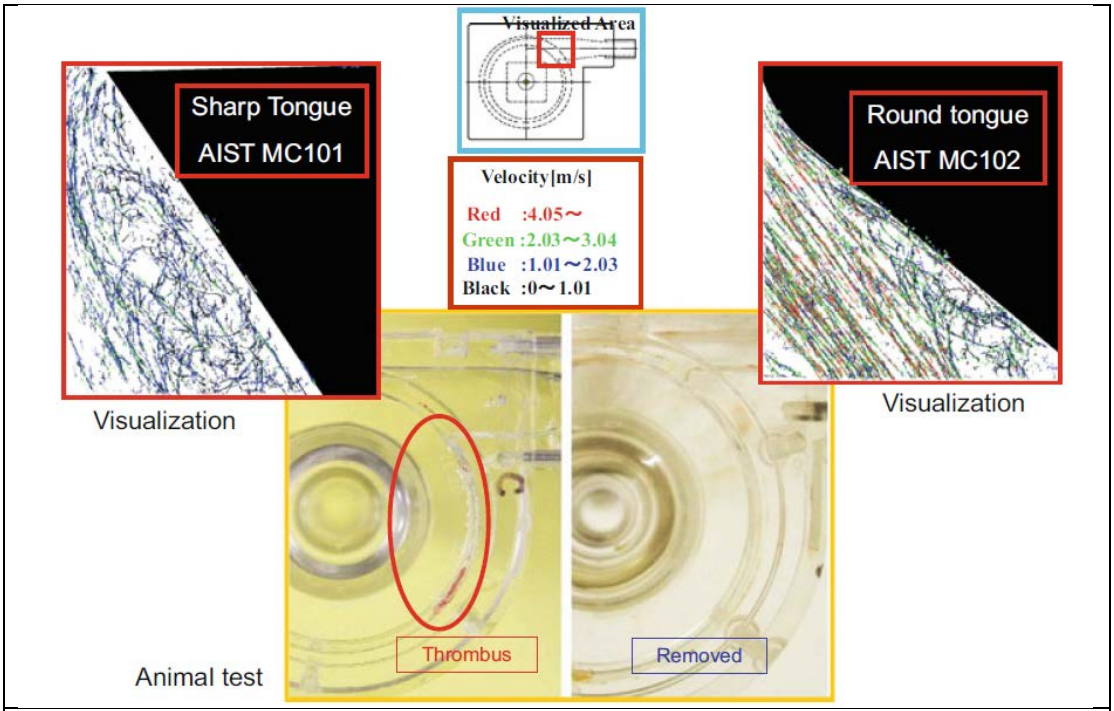

Figure 13: A flow visualization result for tongue regions

Flow visualization was conducted for 300 % scale-up model of the SunMedical centrifugal VAD (Figure 14). The flow visualization revealed a sufficient blood wash between rotating vanes and a stationary shaft.

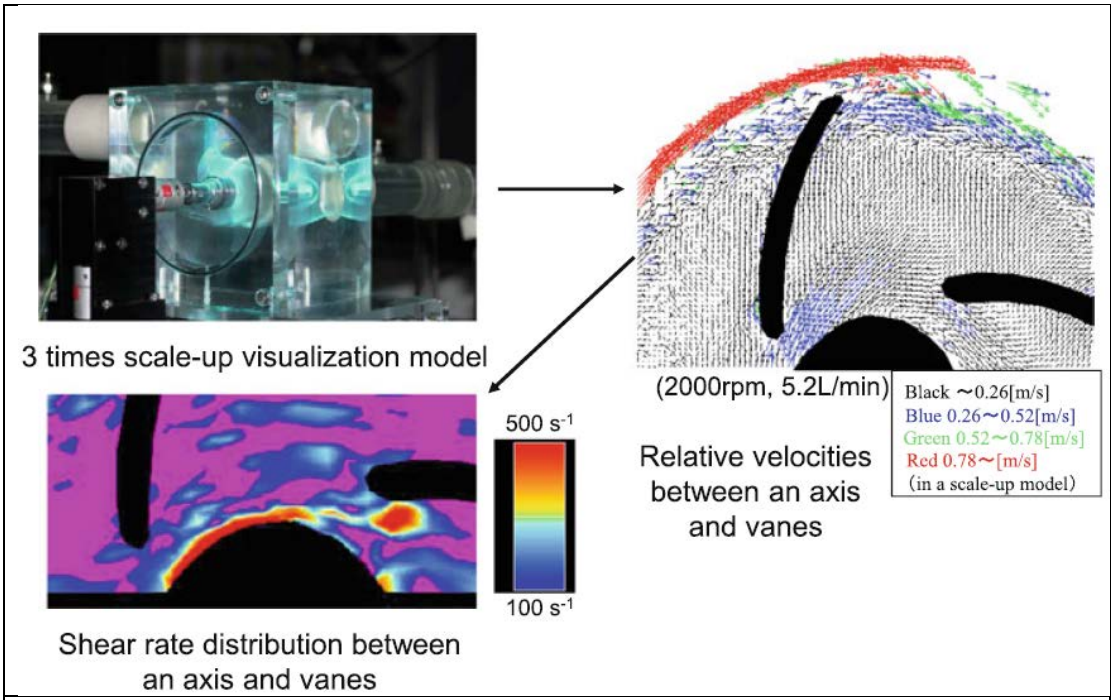

Figure 14: Flow visualization for EVAHEART.

4.3 Visualization Regarding Washout Hole Flow

Around a pivot bearing, blood wash is necessary. Though the tangential flow is accelerated to the tip of impeller and most of them go to the outlet, some of them returns to inlet direction through the top gap or the bottom gap, keeping its angular momentum, namely (velocity x radius), constant. If we see the flow from the side carefully, radially returning flow to the center, so-called secondary flow, may be seen through precise flow visualization analysis. Figure 15 shows that the secondary flow does not reach the pivot at the center for washout holes whose diameter is 9 mm and 8 mm, but it reaches the pivot for those with 7 mm and 6 mm diameter. It was found that the blood wash improves when the washout hole diameter is less than 7 mm.

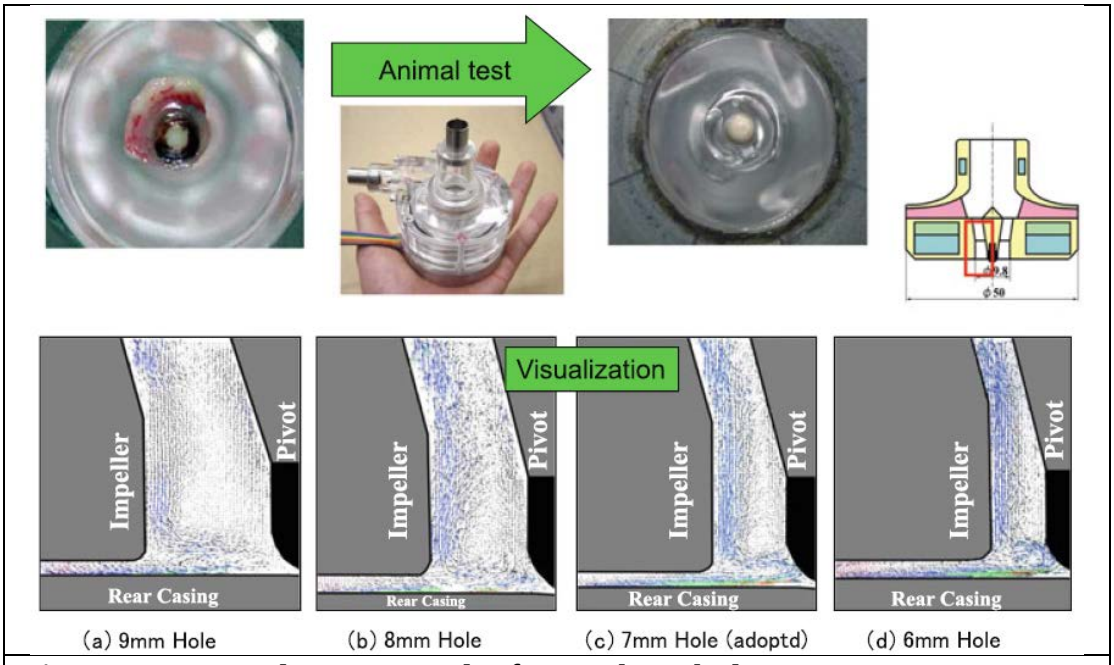

Figure 15: Visualization results for washout hole regions

Second interesting result of flow visualization regarding washout flow is a relative tangential velocity through the top gap or the bottom gap of the impeller. As I wrote, the flow at the impeller tip returns to the center keeping the momentum, namely increasing the tangential velocity. Then the tangential flow reaches the impeller rotational velocity, and the relative velocity between the impeller and the blood becomes zero at a certain radius.

4.4 Computational Fluid Dynamic (CFD) Analysis

The purpose of a computational fluid dynamic (CFD) analysis is to assess hydraulic performance, risk of hemolysis/thrombus formation, or risk of cavitation.

a) Device hydraulic performance: A device design can be evaluated in producing specified hydraulic output within acceptable efficiency.
b) Risk of hemolysis or thrombus formation: Shear stress, exposure time, and their history for blood cells inside the device that could cause blood trauma can be evaluated. Separation and stagnation zones are to be analyzed associated with a risk of thrombus formation.
c) Risk of cavitation: The risk of air emboli, blood cell damage, and blood contacting surfaces damage associated with possible low-pressure zones inside the device can be evaluated.

However, the use is limited to the design stage and to the relative value evaluation since the absolute values need careful validation.

The following items govern the results of CFD analyses:

1) Mesh/grid generation such as mesh size.
2) Used mathematical model such as k-ε turbulence model or laminar flow model.
3) Boundary conditions and initial conditions.

Separate evaluation should be conducted with regard to the following items:

1) Validation (code verification and solution verification).
2) Error analysis (uncertainty quantification).
3) Sensitivity analysis with respect to input parameters.

Since the CFD analysis often fails in obtaining correct pressures or stresses, pressure related evaluation such as pump pressure validation needs to be conducted.

Figure 16 represents a CFD analysis for a velocity profile of the EVAHEART ventricular assist system.

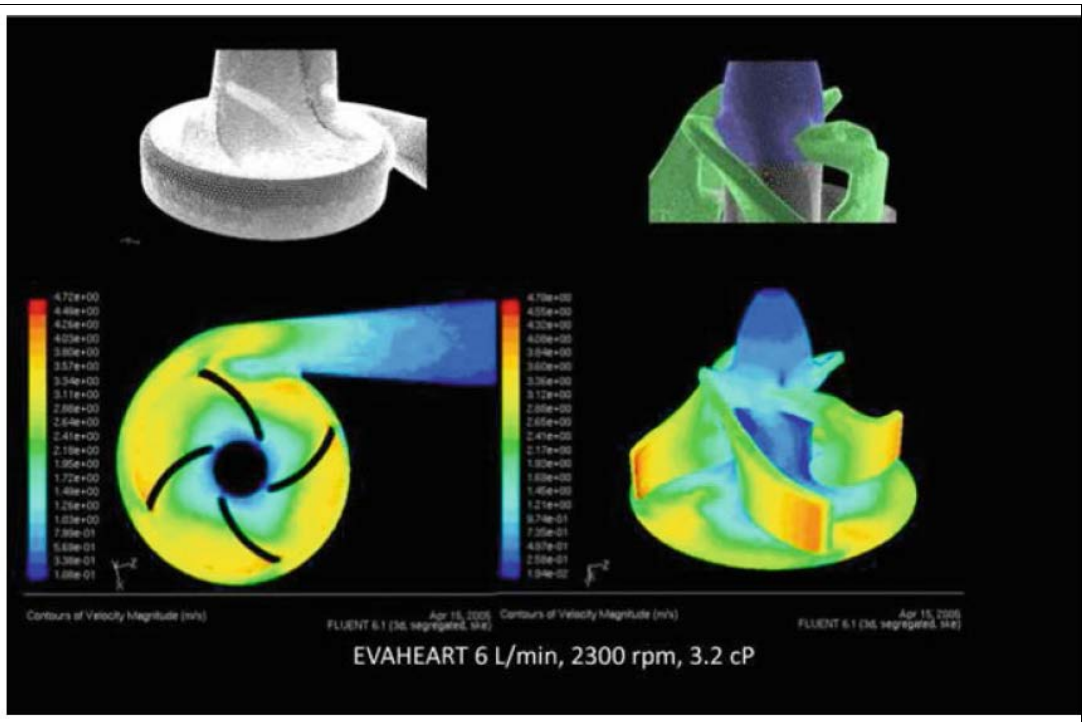

Figure 16: Velocity profile based on computational fluid dynamic (CFD) analysis for EVAHEART

5 Material Selection

5.1 Pump Material

Pump materials have been selected based on both hemocompatibility and structural strength.

For pulsatile TAHs/VADs, polyurethane is often used as pump material because of possessing both hemocompatibility and structural strength. Polytetrafluoroethylene (PTFE) is also used for endovascular grafts.

For extracorporeal rotary pumps, polycarbonate is often used as short-term hemocompatible/structural material because of the toughness against impact and the transparency for observation of blood.

At present for almost all implantable rotary VADs, titanium or titanium alloy as Ti-6Al-4V polished to submicron surface roughness, are used as pump material because other metals have been reported a certain lack of biocompatibility.

Not much new materials have been introduced since getting approval to a new material needs clinical evidences.

5.2 Coating Material

Typical hemocompatible coating material is heparin and 2-methacryloyloxyethyl phosphorylcholine (MPC) polymer. Diamond-like carbon (DLC) can also be coated on hard materials. Heparin coating is used for DuraHeart and MPC polymer coating is used for EVAHEART. On the other hand, Avcothane was coated on segmented polyurethane for pulsatile VADs.

5.3 Bearing Material

A comparative study for materials against rotational wear will be explained here.

To compare the bearing materials, a pivot bearing was modeled as a ball and a plate, and the rotating wear tests were conducted with a rotating wear machine. The ball was attached to a rotating shaft through a Teflon socket, and a cubic receptor was inserted into a stationary square pit in a vessel and axially loaded. They were dipped in a small saline vessel whose temperature was kept at 370C. To prevent splash several fins and a cover plate were provided to the vessel. The rotational speed of a ball was kept at 2000 rpm and the axial load to a receptor was kept at 1 kg or 2 kg. The dried weights of balls/sockets and receptors were measured before a test using a precise balance whose accuracy was þ1 μg. Each rotational wear test was conducted for 16 h. After the test, the dry weights of the components were measured again and the weight losses were evaluated.

Four kinds of ceramics (Si3N4, SiC, Al2O3, and ZrO2) in diameter of 1.59, 3.18, and 3.97 mm were used for pivot balls. Two kinds of materials (Si3N4 and Ultra high molecular weight polyethylene (UHMWPE)) were used for pivot receptors whose size were 6×6×4.9 mm.

First wear vs. time was measured by stopping the apparatus at each sampling time (Figure 17). It was found that the loss of weight was almost linear with respect to time.

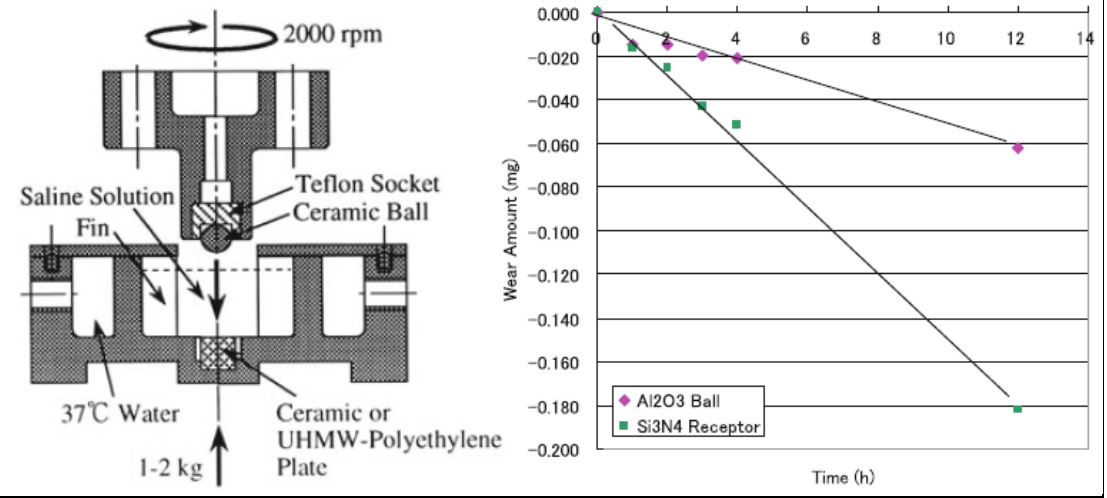

Figure 17: Time history for rotating wear of pivot materials

5.4 Durability Testing

To evaluate system reliability, a closed circuit is filled with a suitable liquid at 37^0C and the test was continued for a target duration. The testing concept and method are described in ISO 14708-5. System reliability is defined as the probability of a system to perform its function for a specified period of time under stated conditions (for example, the demonstrated reliability of the VAD system shall be X with at least Y confidence for a Z year mission life). The number of systems to be tested under controlled in vitro conditions shall be statistically justified to demonstrate that the stated reliability specifications are met. Statistical methods to be employed in the analysis of the reliability test results shall be described. An example of such a statistical justification is a Weibull calculation.

All implanted components shall be tested in a simulated physiological environment, such as a pH buffered, temperature controlled, saline filled tank, and operated within a pulsatile mock circulatory loop. If a pulsatile mock loop is not to be used, a scientific justification shall be provided that lack of pulsatility will not invalidate the test.

For example, a monopivot centrifugal pump, pivot wear was measured continuously for 4 weeks as the distance between the upper casing and the upper impeller surface, using a laser focus displacement meter (Figure 18).

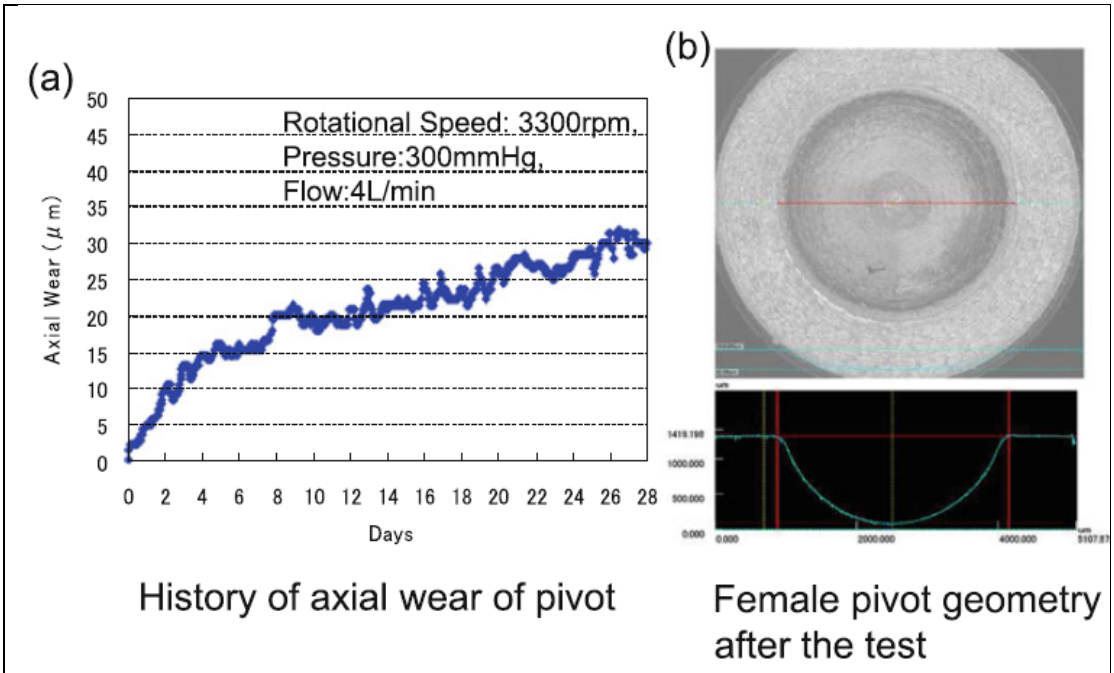

Figure 18: Durability testing for a surgical centrifugal pump

Another example is a durability testing with pulsatile flow of 0–10 L/min was conducted for 2 years with eight axial flow pumps developed in a NEDO project (Figure 19).

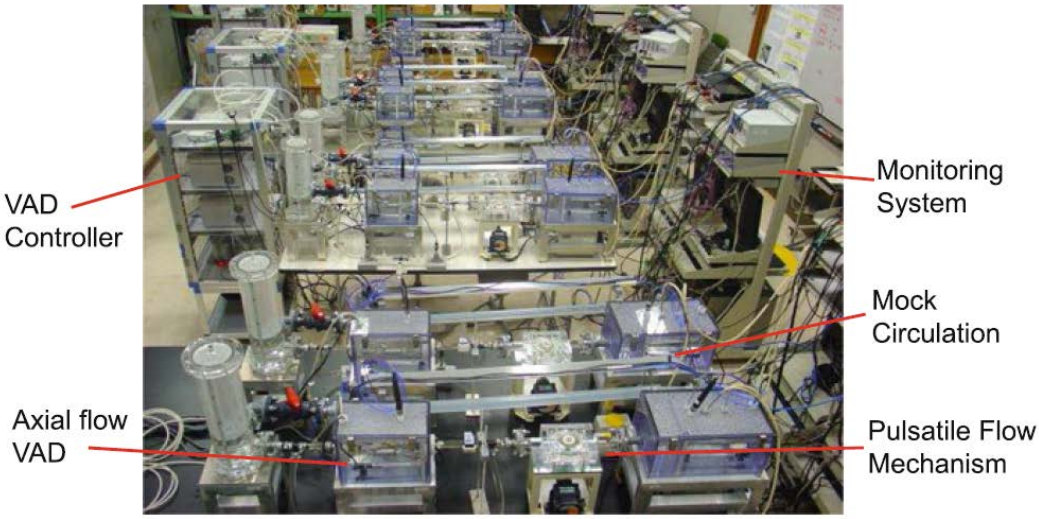

Figure 19: Durability testing with a pulsatile flow for an axial flow VAD, 8 systems for 2 years.